Dyes and Pigments 96 (2013) 52–58

Contents lists available at SciVerse ScienceDirect

Dyes and Pigments

journal homepage: www.elsevier.com/locate/dyepig

Tetracationic fluorinated zinc(ii)phthalocyanine: Synthesis, characterization and DNA-binding properties

Mukaddes Özçeşmeci [a], Özgür Bülent Ecevit [b], Serdar Sürgün [a], Esin Hamuryudan [a,*]

[a] Department of Chemistry, Istanbul Technical University, Maslak, 34469 Istanbul, Turkey
[b] Department of Science, Borough of Manhattan Community College, City University of New York, 10007 NY, USA

ARTICLE INFO

Article history:
Received 5 April 2012
Received in revised form
22 June 2012
Accepted 25 June 2012
Available online 14 July 2012

Keywords:
Fluorinated phthalocyanines
Quaternization
Calf thymus DNA
Nucleophilic substitution
Solubility
Aggregation

ABSTRACT

Selective replacement of the *p*-fluorine atom of 4-(2′,3′,4′,5′,6′-pentafluorobenzyloxy) phthalonitrile with N,N-dimethylaminoetanethiol gave 4-[2′,3′,5′,6′-tetrafluoro-4′-(2-dimethylaminoetanethio)benzyloxy] phthalonitrile. A peripherally tetra-substituted zinc(II) phthalocyanine was achieved by tetramerization of the new perfluorobenzyloxyphthalonitrile in the presence of zinc acetate. The zinc derivative was quaternized with methyl iodide to afford a water-soluble product. The new compounds were characterized by using elemental analyses, ^{1}H NMR, ^{19}F NMR, UV–vis and FT-IR spectroscopy and mass spectrometry. The interaction between the quaternized zinc phthalocyanine and calf thymus DNA was investigated in tris buffer (pH 7.4) by absorption and fluorescence spectroscopy. Upon addition of the quaternized zinc phthalocyanine, a change in the thermal denaturation profile of DNA was observed.

1. Introduction

Phthalocyanines represent an important class of functional dyes [1]. In addition to their use as advanced materials in various fields, these macrocyclic compounds have also found application in medicine. Owing to their strong and long-wavelength absorptions, high efficiency at generating reactive oxygen species, and ease of chemical modification, phthalocyanines have emerged as a promising class of second-generation photosensitisers for photodynamic therapy (PDT) of cancer [2]. Fluorinated MPcs are currently receiving a great deal of attention [3]. The presence of fluorine in the structure of a photosensitizer may enrich it with required pharmacokinetic features. Photostability, high level of singlet oxygen production, lipophilicity and selective accumulation in tumor cells have made the fluorinated porphyrinoids potential entities for photodynamic therapy [4].

Cancer is one of the leading causes of death in the world. Although there are exciting developments in the personalized cancer therapy, such drugs currently represent only a small percentage of the total anticancer agents. Since the molecular recognition of DNA is of fundamental importance to life, the interaction and reaction of metal complexes with DNA continues to be an important area of research. DNA is highly negatively charged and it interacts strongly with oppositely charged species. Cationic porphyrins, phthalocyanines, and their analogs have long been of interest for their interactions with DNA because of their role in the human body, ability to accumulate in many kinds of cancer cells, as well as their magnetic and optical properties. Studies on the interaction of cationic phthalocyanines and their analogs with DNA have received interest in recent years [4–12]. Water soluble cationic phthalocyanines and metallophthalocyanines and their binding to DNA have become important subjects of interest in the search of new DNA-targeting drugs [13,14].

Phthalocyanines are hardly soluble in common solvents, because of their large structures. This causes difficulties in their separation or identification and limits their potential applications in medicine [4]. Significant effort and resources have been utilized to introduce various fluorine containing groups to the periphery of these macrocycles in order to overcome these limitations [15–25].

Moreover, an enhanced solubility of fluorinated phthalocyanines was found to simplify preparation of various drug formulations, including emulsions and nanoparticles. The presence of both superhydrophobic fluorine and hydrophilic N–H groups in the phthalocyanine structure appears to enrich it simultaneously with water solubility [26,27]. Aggregation is also a well-known phenomenon in phthalocyanine chemistry. However, bulky

* Corresponding author. Tel.: +90 212 285 6826; fax: +90 212 285 6386.
E-mail address: esin@itu.edu.tr (E. Hamuryudan).

0143-7208/$ – see front matter © 2012 Elsevier Ltd. All rights reserved.
http://dx.doi.org/10.1016/j.dyepig.2012.06.018

fluorinated substituents on peripheral sites can reduce interactions between phthalocyanine molecules, lowering their aggregation and self-oxidation tendencies [4].

During the last few years we have focused on the preparation of fluorine containing groups introduced to the periphery of phthalocyanines. The introduction of fluoro-substituents on the phthalocyanine improves its solubility in common solvents and enhances electrochemical, spectroelectrochemical and optical properties [15–20]. We report herein the synthesis, characterization and DNA-binding properties of new organo-soluble and water soluble zinc phthalocyanines bearing functionalized polyfluorinated substituents.

2. Experimental

2.1. Materials

Calf-thymus DNA and all other analytical grade chemicals were purchased from Merck Chemicals and Sigma–Aldrich Chemicals. All solvents were dried and purified as described by Perrin et al. [28]. All solutions for DNA-binding studies were prepared using purified water by the Millipore Milli-Q Water system. 4-Nitrophthalonitrile and 4-(2′,3′,4′,5′,6′-pentafluorobenzyloxy) phthalonitrile were prepared according to the reported procedures [15,29]. Silica gel (Kieselgel 60, 200–400 mesh) was used in the separation and purification of compounds by column chromatography. The homogeneity of the products was tested in each step by TLC.

2.2. Equipment

^{1}H NMR spectra were recorded on a Bruker 250 MHz spectrometer using TMS as internal reference. ^{19}F NMR spectrum was recorded on a Varian Unity Inova 500 MHz NMR. IR spectra were recorded on a Perkin–Elmer Spectrum One FT-IR (ATR sampling accessory) spectrophotometer. Electronic spectra were recorded on a Scinco LabProPlus UV/vis spectrophotometer. Absorbance and fluorescence spectra for DNA-binding experiments were recorded in a quartz cuvette using Hitachi U-2910 and FluoroMax-4 (Horiba Jobin Yvon), respectively. Mass spectra were performed on Varian 711 and Bruker microflex LT MALDI-TOF MS mass spectrometers. The isotopic patterns for all assigned signals are in agreement with the calculated natural abundance. Data have been given for the most abundant isotope only.

2.3. Synthesis

2.3.1. Synthesis of 4-[2′,3′,5′,6′-tetrafluoro-4′-(2-dimethylaminoetanethio)benzyloxy] phthalonitrile (**1**)

4-(2′,3′,4′,5′,6′-pentafluorobenzyloxy)phthalonitrile (1 g, 3.085 mmol) was dissolved in dry DMF (20 mL) under nitrogen atmosphere and N,N-dimethylaminoethanethiol (0.320 g, 3.085 mmol) was added to the solution. After stirring 10 min, finely ground anhydrous K_2CO_3 (0.639 g, 4.628 mmol) was added portionwise within 2 h with efficient stirring. The reaction mixture was stirred under nitrogen at 50 °C for 48 h. Then the solution was poured into ice-water (200 mL). The precipitate was collected by filtration, washed first with water until the filtrate was neutral and then extracted with chloroform (3 × 200 mL); the chloroform extracts were combined, dried over $MgSO_4$, and the solvent was removed at reduced pressure. The desired product was isolated by column chromatography with silica gel using methanol/chloroform (1:100) as eluent. Yield: 0.189 g (15%), mp: 53 °C. Anal. calcd. for $C_{19}H_{15}F_4N_3OS$: C, 55.74; H, 3.69; N, 10.26%. Found: C, 55.59; H, 3.42; N, 10.43. IR ν_{max}, cm^{-1}: 3088 (Ar–CH), 2918–2776 (alkyl CH), 2231 (C≡N), 1250 (C–O–C); ^{1}H NMR ($CDCl_3$), (δ, ppm): 7.74 (d, J = 8.64 Hz, H, Ar–H), 7.34 (s, H, Ar–H), 7.28 (d, J = 8.70 Hz, H, Ar–H), 5.21 (s, 2H, OCH_2), 3.01 (t, 2H, SCH_2), 2.54 (t, 2H, NCH_2), 2.23 (s, 6H, NCH_3); ^{19}F NMR (acetone-d_6), (δ, ppm): −144.1 (d-*o*-fluorine), −164.4 (q-*m*-fluorine); MS (ESI$^+$): m/z 378.6 $[M\text{-}2CH_3]^+$.

2.3.2. Synthesis of 2,9(10), 16(17), 23(24)-tetrakis-[2′,3′,5′,6′-tetrafluoro-4′-(2-dimethylaminoetanethio) benzyloxy] phthalocyaninato zinc(II) (**2**)

A mixture of **1** (0.150 g, 0.366 mmol), anhydrous $Zn(CH_3COO)_2$ (0.017 g, 0.0915 mmol), and anhydrous DMF (2 mL) were mixed in a glass tube which was sealed under nitrogen. After the reaction mixture was heated and stirred at 140 °C for 2 days, the mixture was cooled to room temperature. Then it was poured into ice water (200 mL). The creamy precipitate was washed with water and dried *in vacuo*. The green product was isolated by column chromatography with silica gel using THF/hexane (5:2) as eluent. Yield: 0.070 g (45%), m.p: >200 °C. Anal. calcd. for $C_{76}H_{60}F_{16}N_{12}O_4S_4Zn$: C, 53.60; H, 3.55; N, 9.87%. Found: C, 53.71; H, 3.63; N, 9.92. IR ν_{max}, cm^{-1}: 2952–252 (alkyl CH), 1217 (C–O–C); ^{1}H NMR ($CDCl_3$), (δ, ppm): 7.74 (d, J = 8.32 Hz, 4H, Ar–H), 7.53 (s, 4H, Ar–H), 7.39 (d, J = 8.30 Hz, 4H, Ar–H), 5.17 (s, 8H, OCH_2), 3.30 (t, 8H, SCH_2), 2.91 (t, 8H, NCH_2), 2.80 (s, 24H, NCH_3). ^{19}F NMR ($CDCl_3$), (δ, ppm): −143.61 (m, 8F, *o*-fluorine), −164.70 (m, 8F, *m*-fluorine). UV–vis (THF): λ_{max}/nm (log ε): 350 (4.28), 676 (4.57). MS (MALDI-TOF MS) m/z: 1654.47 $[M\text{-}3CH_3]^+$.

2.3.3. Synthesis of 2,9(10), 16(17), 23(24)-tetrakis-[2′,3′,5′,6′-tetrafluoro-4′-(2-dimethylaminoetanethio)benzyloxy] phthalocyaninato zinc(II)tetraiodide (**3**)

Compound **2** (0.030 g, 0.018 mmol) was dissolved in chloroform (30 mL) and methyl iodide (0.010 mg, 0.072 mmol) was added to this solution. The reaction mixture was stirred first at 50 °C for 3 h and then at room temperature for 20 h. The resulting suspension was filtered off, washed with $CHCl_3$ and dried. Yield: 0.020 g (48%), m.p: >200 °C. Anal. calcd. for $C_{80}H_{72}F_{16}N_{12}O_4S_4I_4Zn$: C, 42.31; H, 3.20; N, 7.40%. Found: C, 42.43; H, 3.53; N, 7.58. IR ν_{max}, cm^{-1}: 2956–2776 (alkyl CH), 1220 (C–O–C); ^{19}F NMR (*d*-DMSO), (δ, ppm): −145.27 (m, 8F, *o*-fluorine), −161.75 (m, 8F, *m*-fluorine). ^{1}H NMR (*d*-DMSO), (δ, ppm): 9.32–9.04 (m, 8H, Ar–H), 7.86 (s, 4H, Ar–H), 5.83 (s, 8H, OCH_2), 3.55 (t, 8H, SCH_2), 3.31 (s, 36H, NCH_3), 2.97 (s, 8H, NCH_2). UV–vis (DMSO): λ_{max}/nm (log ε): 360 (4.25), 683 (4.55). MS (MALDI-TOF MS) m/z: 2181.66 $[M\text{-}6CH_3]^+$, 1420.23 $[M\text{-}6CH_3I]^+$.

2.4. DNA-binding studies

2.4.1. Absorbance and fluorescence studies

All titrations for DNA-binding experiments were conducted at pH 7.4 in a 10 mM Tris buffer containing 50 mM NaCl. The final concentration of ct-DNA was 1–20 mM. The concentration of ct-DNA was determined by UV absorbance at 260 nm using the molar absorptivity constant of 13,200 M^{-1} cm^{-1}. In order to determine dilution effects, a control experiment was performed in which the DNA solution was replaced by buffer solution. Absorption spectra were recorded in the region of 350–825 nm, and fluorescence spectra were recorded in the region of 660–760 nm after excitation at 655 nm. Titrations of the Pc with ct-DNA were performed by adding small aliquot (10 μL) of a concentrated DNA solution to the Pc solution at constant concentration. All solutions were allowed to equilibrate for 10 min before measurements were recorded.

2.4.2. Thermal-denaturation studies

Ct-DNA and Pc in buffer solution were heated in the temperature range of 30 °C–85 °C at a rate of 0.2°/min. Melting

temperatures were monitored at 260 nm wavelength using Hitachi U-2910 spectrophotometer.

3. Results and discussion

3.1. Synthesis and characterization

The synthetic procedure for the new compounds is outlined in Scheme 1. The phthalonitrile derivative **1** was obtained by base-catalyzed aromatic nucleophilic displacement of fluoride ion from 4-(2′,3′,4′,5′,6′-pentafluorobenzyloxy)phthalonitrile with the −SH function of N,N-dimethylaminoethanethiol using K_2CO_3 as the base in dry DMF at 50 °C under N_2 for 48 h (Scheme 1). The substitution regioselectivity was always quite high only at the *para*-fluorine of pentafluorophenyl group with O−, S− or N− nucleophiles [30].

Cyclotetramerization of the dinitrile **1** to the tetra-substituted zinc phthalocyanine (**2**) was accomplished in the presence of anhydrous $Zn(CH_3COO)_2$ in DMF at 140 °C for 2 days in a sealed tube. Compound **2** was isolated by column chromatography on silica gel using THF/hexane (5:2) mixtures as an eluent. As a natural consequence of the presence of single substituents on each benzo group, the phthalocyanine **2** is a mixture of four structural isomers (D_{2h}:C_s:C_{2v}:C_{4h}). The presence of isomers might be verified by the slight broadening encountered in the UV−vis absorption bands and broadening of the signals in the ^{1}H NMR spectrum. No attempt was made to separate the isomers of **2**. Tetra-cationic zinc phthalocyanine (**3**) was obtained from the reaction of corresponding phthalocyanine (**2**) with methyl iodide in $CHCl_3$ (Scheme 2) [31–36]. With regard to the solubility of phthalocyanines, the green product **2** is soluble in most of the polar organic solvents such as $CHCl_3$, CH_2Cl_2, THF, acetone; whilst the cationic derivative **3** is fully soluble in water and DMSO as expected.

Elemental analysis results and the spectral data (FT-IR, ^{1}H NMR, ^{19}F NMR, UV−vis and MS) for the newly synthesized compounds were consistent with the assigned formulations.

In the FT-IR spectrum of compound **1**, stretching vibrations of C≡N groups at 2231 cm^{-1}, aliphatic CH groups at 2918−2776 cm^{-1}, aromatic CH groups at 3088 cm^{-1}, and ether (C−O−C) units at 1250 cm^{-1} appeared at expected frequencies. In the ^{1}H NMR spectrum of compound **1** in $CDCl_3$, the aromatic protons are present as a doublet, singlet, doublet at δ: 7.74, 7.34, 7.28 ppm, respectively. The CH_2 protons of pentafluorobenzyl group appear at δ: 5.21 ppm as a singlet and the aliphatic protons of the side chains of **1** exhibited the $-SCH_2$ protons as a triplet at δ: 3.01 ppm. The $-NCH_2$ protons resonate at δ: 2.54 ppm and $-NCH_3$ protons at δ: 2.23 ppm as a singlet.

The ^{19}F NMR spectrum of **1** in acetone-d_6 is revealed only two fluorine peaks at δ: −144.1 and −164.4 ppm, thus supporting the idea that *para*-fluorine atom was replaced with 2-dimethylaminoetanethio group. Phthalocyanines **2** and **3** also have very similar ^{19}F NMR spectra for the fluorinated peripheral substituents. In the ^{19}F NMR spectrum of compound **2** in $CDCl_3$, the *ortho* and *meta* fluorine atoms are present as a multiplet at δ: 143.61 and 164.70 ppm, respectively. In *d*-DMSO compound **3** gives the signals as a multiplet at δ: 145.27 and 161.75 ppm, respectively.

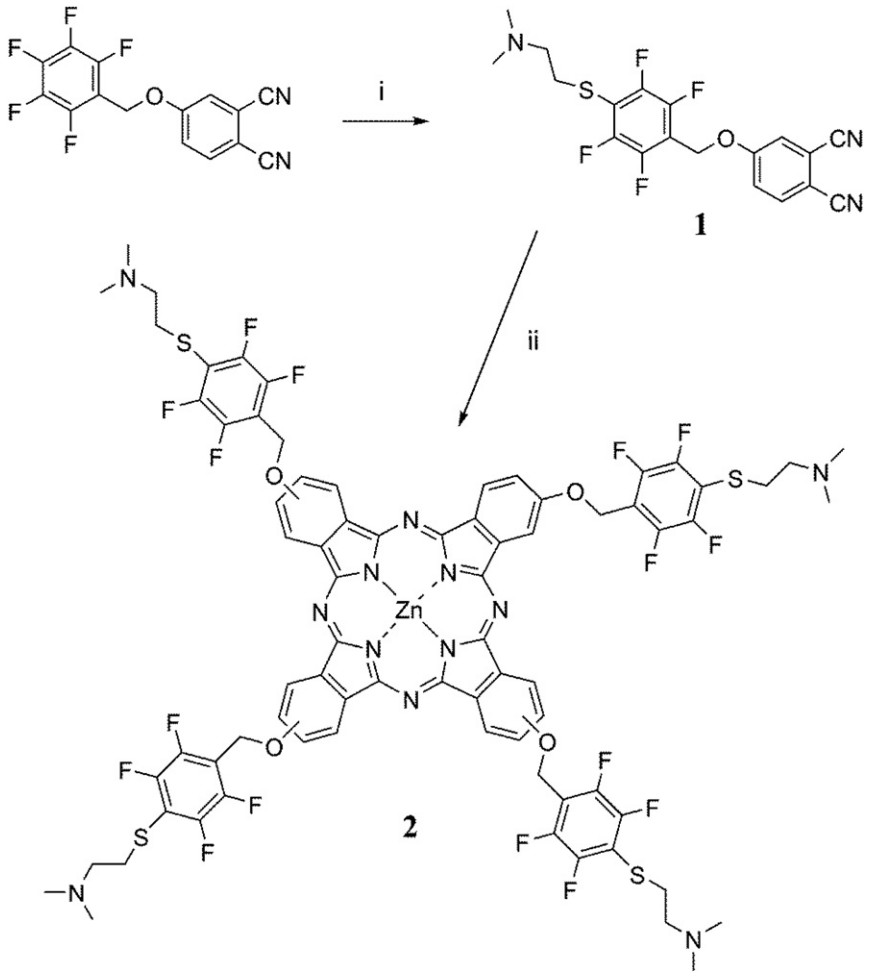

Scheme 1. Synthetic route of the phthalonitrile derivative (**1**) and ZnPc (**2**); (i) N,N-dimethylaminoethanethiol, DMF and K_2CO_3; (ii) $Zn(CH_3COO)_2$ and DMF.

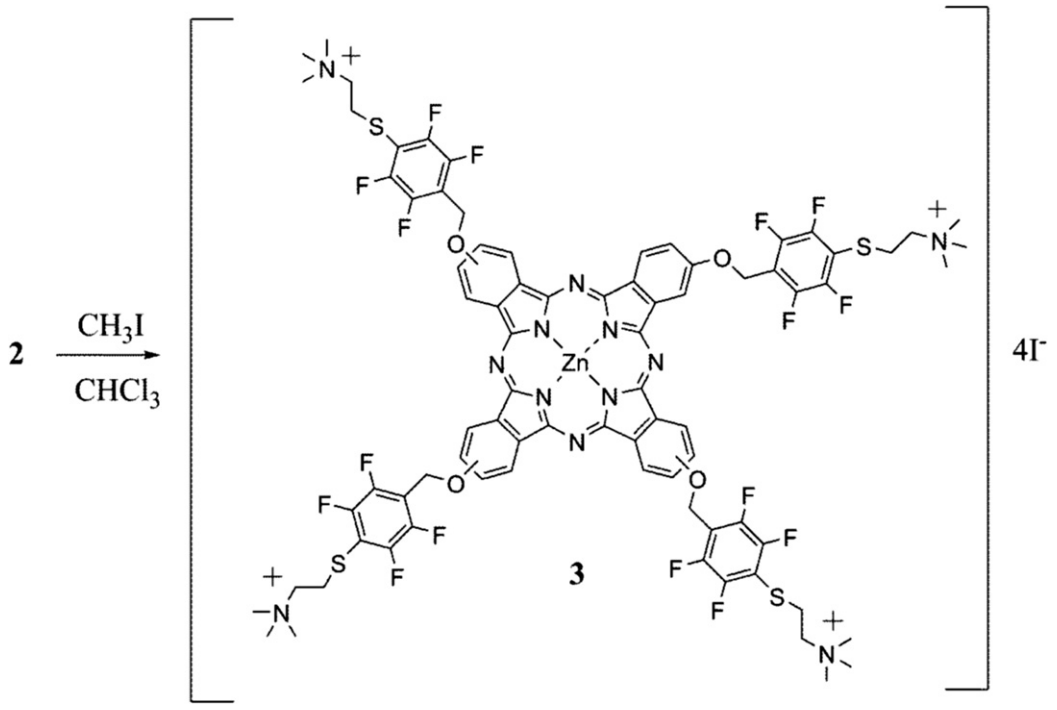

Scheme 2. Synthetic route of the quaternized ZnPc (3).

The cyclotetramerization of compound **1** can be seen clearly by the absence of the C≡N peaks at 2231 cm^{-1}, on the FT-IR spectrum on formation of compound **2**. The FT-IR spectrum of **2** showed similar characteristics. Also, no major change was found in the FT-IR spectrum of **3** after quarternization.

The ^{1}H NMR spectrum of tetra substituted zinc(II) phthalocyanine derivative (**2**) was almost identical with that of the starting compound **1** except for some signal broadening and some small shifts in the positions of some signals. It is probable that the phthalocyanine derivative obtained as a mixture of positional isomers which are expected to show chemical shifts that differ slightly from each other.

The mass spectrum of **1** was obtained by MS (ESI) technique. In the mass spectrum of **1**, fragment ion corresponding to the loss of $[M\text{-}2CH_3]^+$ at *m*/*z*: 378.6 was easily identified. Also, MALDI-TOF MS technique was used to identify compound **2** and **3**. In the mass spectrum of **2**, the fragment ion peak corresponding to the loss of $[M\text{-}3CH_3]^+$ was observed at *m*/*z*: 1654.47. In the case of **3**, the fragment ion peaks corresponding to the loss of $[M\text{-}6CH_3]^+$ and $[M\text{-}6CH_3I]^+$ were observed at *m*/*z*: 2181.66, 1420,23 respectively.

Electronic spectra are especially fruitful to establish the structure of the phthalocyanines. The phthalocyanines exhibit typical electronic spectra with two strong absorption regions, one in the UV region at about 300–400 nm (B-band) and the other one is in the visible region at 600–700 nm (Q-band), both correlate to π–π^* transitions. The characteristic Q-band transition of **2** was observed as a single band at 676 nm in THF. In the spectrum of the quaternized zinc phthalocyanine (**3**) in DMSO the Q-band was observed at 683 nm. B-bands of these phthalocyanines (**2**–**3**) appeared at around 350–360 nm. Generally in Pcs increasing the concentration leads to aggregation, which is easily observed by the values of the Q band absorptions. In this study, complex **2** did not show aggregation in THF at different concentrations, because of the bulky nature of 2′,3′,5′,6′-tetrafluoro-4′-(2-dimethylaminoetanethio)benzyloxy groups on the peripheral sites of macrocycle ring [20]. Fig. 1 shows the changes in the visible spectrum of **2** in THF with concentration. The Beer-lambert law was obeyed for compound **2** in the concentrations ranging from 2.0×10^{-6} to 2.0×10^{-5} mol dm^{-3} at maximum absorption ($\lambda = 676$ nm). The Beer-Lambert relationship is shown as an inset for **2** in Fig. 1. As the concentration is increased, the absorption maxima of the Q band also increased and the blue shift of Q band absorptions is not observed.

3.2. Aggregation behavior of quaternized zinc phthalocyanine (3) in aqueous solutions

The UV–vis spectrum of the quaternized zinc phthalocyanine (**3**) in DMSO is very similar to corresponding non-quaternized derivative **2** in THF. However, the electronic spectrum of **3** in water showed some differences from that in DMSO as a result of

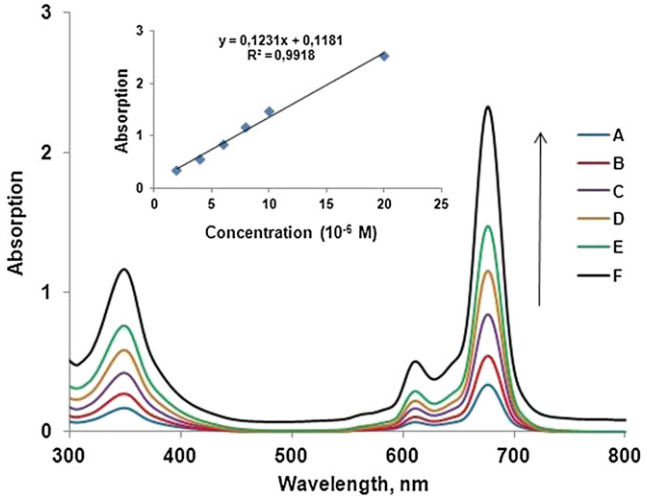

Fig. 1. UV–vis spectra of **2** in THF at different concentrations: 2×10^{-6} (A), 4×10^{-6} (B), 6×10^{-6} (C), 8×10^{-6} (D), 1×10^{-5} (E), 2×10^{-5} (F) mol dm^{-3}.

differing solvent. First, the B-bands are slightly shifted to shorter wavelength. Second, the intensity of the Q-bands is much lower. Third, for **3**, the Q-bands absorption is present as a shoulder, while the absorption of the aggregated species around 645 nm is the main peak (Fig. 2) [37,38].

Aggregation behavior of Pc is depicted as a coplanar association of rings progressing from monomer to dimer and higher order complexes and it is dependent on concentration, nature of solvent and substituents, metal ions and temperature [19,39,40].

Aggregation is not desired in MPc complexes since aggregates are generally photoinactive. This problem is particularly serious in polar media such as water, which tends to self-associate and repel the hydrophobic π systems to form aggregates. Therefore, hydrophilic and nonaggregated phthalocyanines have special importance and have received much current attention. One of the strategies to reduce the aggregation of phthalocyanines in aqueous media involves the use of surfactants or other substances which can create a microheterogeneous environment such as a micelle or liposome. It has been found that phthalocyanines exist mainly as monomeric species in these environments, giving a relatively high photoactivity [41]. Addition of a drop of Triton X-100 to an aqueous solution of **3** resulted in the decrease in the high energy band due to the aggregates and the increase in the low energy band due to the monomer (683 nm for **3**) (Fig. 3).

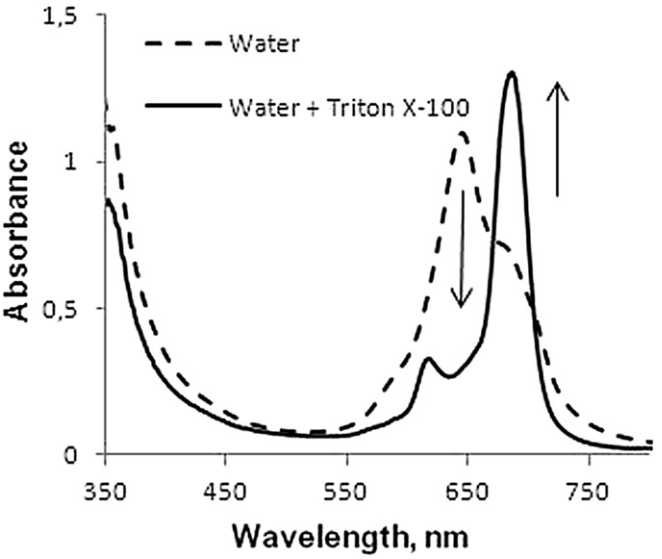

Fig. 3. UV–vis spectra of **3** in water and water containing Triton X-100.

3.3. DNA-binding studies

3.3.1. Absorbance studies

Absorption titration experiments were performed to investigate the binding of Pc to ct-DNA. It is very important to understand the binding modes of Pc to DNA. There are three possible known binding modes of phthalocyanines to DNA: intercalation, external binding and external binding with stacking. Intercalation is the process where the phthalocyanine molecules insert themselves in between base pairs of DNA. In general intercalation involves a relatively hydrophobic, polar, planar region of the DNA binder, but electrostatic, dipole–dipole, and H-binding interactions between the intercalator and DNA are also important. Electrostatic and H-bonding interactions are the main binding forces in external binding. Some of the factors which inhibit intercalation and favor external binding are steric hindrance and lack of planarity [42].

The binding mode of Pc to DNA is one of the crucial factors affecting the degree of the wavelength shift and also whether hypochromism or hyperchromism occurs. A considerable red shift is considered to be indicative of an intercalation as a result of a π–π stacking between DNA bases and Pc. On the other hand, small changes in the absorption spectra usually indicate external stacking or electrostatic binding. In the absorption titration spectrum of **3**, as shown in Fig. 4, a small blue shift and hypochromicity were observed in the Q-band upon addition of various amounts of ct-DNA to **3**. Addition of ct-DNA to **3** caused also a small bathochromic shift in the wavelength maximum of the B-Band, and a decrease in the intensity of the spectrum. The wavelength shifts in the Q and B-Bands were not large enough to be considered indicative of an intercalation. The insignificant blue and red shifts in the Q- and B-Bands, respectively, were attributed to an electrostatic binding between the cationic Pc and the negatively charged DNA phosphate backbone.

3.3.2. Fluorescence studies

In order to calculate the binding constants of Pc to DNA, generally, either fluorescence or absorbance titration is utilized.

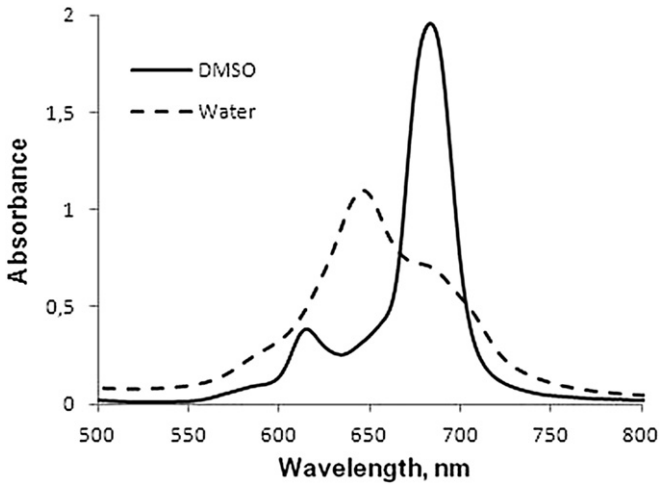

Fig. 2. UV–vis absorption spectra of **3** in water and DMSO.

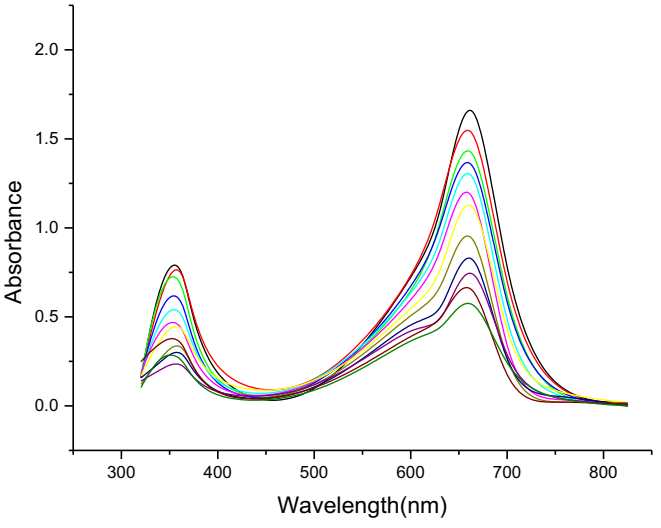

Fig. 4. Absorbance titration spectra of **3** (5 μM) upon addition of increasing amounts of ct-DNA (0, 3, 6, 9, 12, 15, 18, 21, 24, 27, 30, and 33 μM) (from top to bottom).

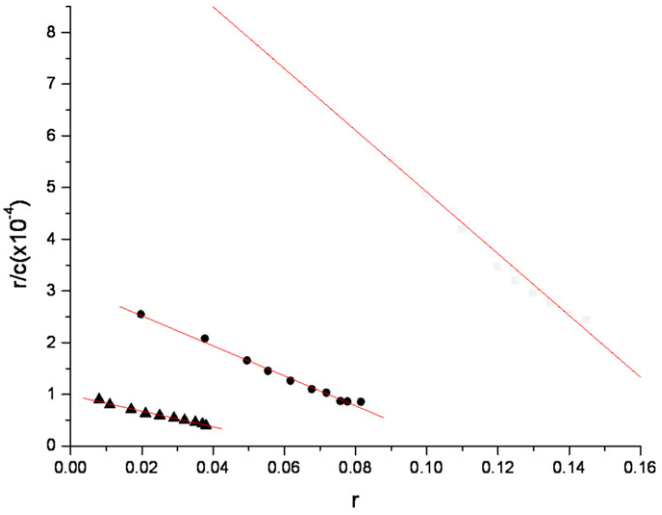

Fig. 5. Scatchard plots obtained from the competitive fluorescence titration data for binding of **3** to DNA. With 2–11 μM ethidium bromide, ■: 0 μM, ●: 0.1 μM, ▲: 0.2 μM.

Absorbance titration data is very useful for determining the absorption coefficient of bound Pc, if the binding mode between the Pc and DNA is intercalative. However, in our experiments, only a small change was observed in the Q and B-Bands of the absorption spectrum upon binding to DNA which suggests a non-intercalating binding mode. Therefore, a fluorescence titration method was used to determine the apparent binding constant (K_{app}). In this method, ethidium bromide, an intercalating agent, is used as a spectroscopic probe and a competitive fluorescence titration is carried out to monitor the decrease in the fluorescence intensity of ethidium bromide bound to DNA in the presence of **3**. The intercalating ability of **3** can be calculated by using the amount of decrease in fluorescence intensity of ethidium bromide bound to DNA. Fluorescence titration data obtained by this method were used for the Scatchard plot analysis shown in Fig. 5. The apparent binding constant of **3** to DNA calculated from the Scatchard plot (6.20×10^5 M^{-1}) is found to be smaller than 10^6, which is an average value for the apparent binding constant of small intercalating compounds. This result suggests that the mode of binding for **3** to ct-DNA is most likely to be non-intercalative.

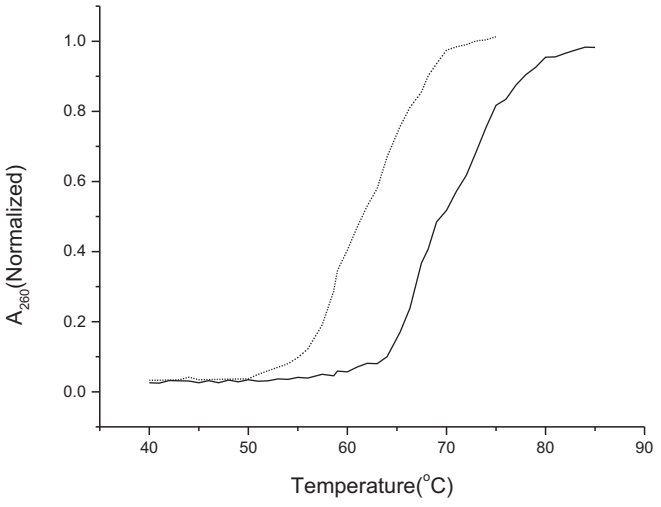

Fig. 6. Thermal denaturation profiles of ct-DNA (dashed) and ct-DNA with **3** (solid).

3.3.3. Thermal-denaturation studies

DNA melting profile is very informative about helix stability. Thermal denaturation studies on DNA in the presence of a ligand can also be employed to differentiate between electrostatic and intercalative binding modes. The difference between the melting temperatures of DNA in a buffer solution and DNA with a ligand is usually large if the binding of the ligand to DNA occurs through intercalation. On the other hand, if the binding mode of the ligand to DNA is non-intercalative, the difference in the melting temperatures is generally smaller. In our experiments, DNA melting profile is found to be sensitive to the addition of **3**, as shown in Fig. 6. Addition of 5 μM of **3**–35 μM of ct-DNA increased the melting temperature of ct-DNA by about 8 °C. This small change in the melting temperature is also indicative of a non-intercalative binding between ct-DNA and **3**.

4. Conclusion

In this work, we have synthesized and characterized a novel Zn phthalocyanine substituted with four 2′,3′,5′,6′-tetrafluoro-4′-(2-dimethylaminoetanethio)benzyloxy substituents on peripheral positions and produced tetra-cationic water soluble Zn phthalocyanine. Using absorption and fluorescence spectroscopic techniques, DNA binding properties of tetra-cationic ZnPc were also investigated and the change in the melting point of DNA was determined with thermal denaturation profiles. Titrametric investigation indicate that electrostatic binding between cationic phthalocyanine and anionic DNA phosphate groups is occurring to a large extend and π–π stacking between DNA and phthalocyanine moieties takes place afterward.

In summary, the findings of this study will help us to enhance our understanding of the binding modes of the phthalocyanines, in particular polyfluorinated substituted metallo-phthalocyanines, to DNA. In addition, these data will form the basis of our research efforts on the use of these novel phthalocyanines as promising candidates in photodynamic therapy.

Acknowledgments

This work was supported by the Research Fund of the Istanbul Technical University.

References

[1] McKeown NB. Phthalocyanine materials. Cambridge: Cambridge University Press; 1998.
[2] Lukyanets EA. Phthalocyanines as photosensitizers in the photodynamic therapy of cancer. J Porphyr Phthalocya 1999;3:424–32.
[3] Qiu T, Xu X, Liu J, Qian X. Novel perfluoroalkyl phthalocyanine metal derivatives: synthesis and photodynamic activities. Dyes Pigm 2009;83:127–33.
[4] Goslinski T, Piskorz J. Fluorinated porphyrinoids and their biomedical applications. J Photochem Photobiol C Photochem Rev 2011;12:304–21.
[5] Asadi M, Safaei E, Ranjbar B, Hasani L. Thermodynamic and spectroscopic study on the binding of cationic Zn(II) and Co(II) tetrapyridinoporphyrazines to calf thymus DNA: the role of the central metal in binding parameters. New J Chem 2004;28:1227–34.
[6] Ozturk R, Kalay S, Kalkan A, Turkan A, Abasiyanik MF, Bayir ZA, et al. DNA and BSA binding studies of novel tetracationic phthalocyanines. J Porphyr Phthalocya 2008;12:932–41.
[7] Duan W, Wang Z, Cook MJ. Synthesis of tetra(trimethylammonio)phthalocyanato zinc tetraiodide, [ZnPc(NMe3)4]I4, and a spectrometric investigation of its interaction with calf thymus DNA. J Porphyr Phthalocya 2009;13:1255–61.
[8] Zhang AM, Huang J, Weng XC, Li JX, Ren LG, Song ZB, et al. A water-soluble, octacationic zinc phthalocyanine as molecular probe for nucleic acid secondary structure. Chem Biodiver 2007;4:215–23.
[9] Kubat P, Lang K, Anzenbacher Jr P, Jursikova K, Kral V, Ehrenberg B. Interaction of novel cationic *meso*-tetraphenylporphyrins in the ground and excited states with DNA and nucleotides. J Chem Soc Perkin Trans 2000;1:933–41.
[10] Monajjemi M, Aghaie H, Naderi F. Thermodynamic study of interaction of TSPP, CoTsPc, and FeTsPc with calf thymus DNA. Biochemistry (Moscow) 2007;72(6):652–7.

[11] Uslan C, Sesalan BŞ. Synthesis of novel DNA-interacting phthalocyanines. Dyes Pigm 2012;94:127–35.
[12] Shuai L, Wang S, Zhang L, Fu B, Zhou X. Cationic porphyrins and analogues as new DNA topoisomerase I and II inhibitors. Chem Biodiver 2009;6:827–37.
[13] Mao JF, Zhang Y, Zhu J, Zhang C, Guo Z. Molecular combo of photodynamic therapeutic agent silicon(IV) phthalocyanine and anticancer drug cisplatin. Chem Commun 2009;8:908–10.
[14] Spesia MB, Caminos DA, Pons P, Durantini EN. Mechanistic insight of the photodynamic inactivation of *Escherichia coli* by a tetracationic zinc(II) phthalocyanine derivative. Photodiag Photodyn Ther 2009;6:52–61.
[15] Selçukoğlu M, Hamuryudan E. Novel phthalocyanines with pentafluorobenzyloxy-substituents. Dyes Pigm 2007;74:17–20.
[16] Koca A, Özkaya AR, Selçukoğlu M, Hamuryudan E. Electrochemical and spectroelectrochemical characterization of the phthalocyanines with pentafluorobenzyloxy substituents. Electrochim Acta 2007;52:2683–90.
[17] Özçeşmeci M, Hamuryudan E. The synthesis and characterization of functionalized polyfluorinated phthalocyanines. Dyes Pigm 2008;77:457–61.
[18] Koca A, Özçeşmeci M, Hamuryudan E. Substituents effects to the electrochemical, and in-situ spectroelectrochemical, behaviors of metallophthalocyanines: electrocatalytic application for hydrogen evolution reaction. Electroanalysis 2010;22(14):1623–33.
[19] Özçeşmeci M, Özçeşmeci İ, Hamuryudan E. Synthesis and characterization of new polyfluorinated dendrimeric phthalocyanines. Polyhedron 2010;29(13): 2710–5.
[20] Özçeşmeci M, Sorar İ, Hamuryudan E. Synthesis, optical and structural studies of tetrakis[4-(2′,3′,4′,5′,6′-pentafluorobenzyloxy)benzyloxy]-substituted metallo-phthalocyanines. Polyhedron 2012;162:154–61.
[21] Gürol İ, Durmuş M, Ahsen V. Photophysical and photochemical properties of fluorinated and nonfluorinated n-propanol-substituted zinc phthalocyanines. Eur J Inorg Chem 2010;2010:1220–30.
[22] Burat AK, Öz ZP, Bayır ZA. Synthesis and electronic absorption studies of novel (trifluoromethyl)phenoxy-substituted phthalocyanines. Monatsh Chem 2012; 143:437–42.
[23] Gerdes R, Lapok L, Tsaryova O, Wöhrle D, Gorun SM. Rational design of a reactive yet stable organic-based photocatalyst. Dalton Trans 2009;7: 1098–100.
[24] Ünlü S, Yaraşır MN, Kandaz M, Koca A, Salih B. Synthesis, spectroscopy and electrochemical properties of highly soluble fluoro containing phthalocyanines. Polyhedron 2008;27:2805–10.
[25] Aggarwal A, Singh S, Zhang Y, Anthes M, Samaroo D, Gao R, et al. Synthesis and photophysics of an octathioglycosylated zinc(II) phthalocyanine. Tetrahedron Lett 2011;52:5456–9.
[26] Minnes R, Weitman H, Lee HJ, Gorun SM, Ehrenberg B. Enhanced acidity, photophysical properties and liposome binding of perfluoroalkylated phthalocyanines lacking C–H Bonds. Photochem Photobiol 2006;82(2):593–9.
[27] Erdoğmuş A, Nyokong T. Synthesis of zinc phthalocyanine derivatives with improved photophysicochemical properties in aqueous media. J Mol Struct 2010;977:26–38.
[28] Perrin DD, Armarego WLF, Perrin DR. Purification of laboratory chemicals. 2nd ed. New York: Pergamon Press; 1985.
[29] Young JG, Onyebuagu W. Synthesis and characterization of di-disubstituted phthalocyanines. J Org Chem 1990;55:2155–9.
[30] Kvicala J, Benes M, Paleta O, Kral V. Regiospecific nucleophilic substitution in 2,3,4,5,6-pentafluorobiphenyl as model compound for supramolecular systems. Theoretical study of transition states and energy profiles, evidence for tetrahedral S_N2 mechanism. J Fluorine Chem 2010;131:1327–37.
[31] Arslanoglu Y, Hamuryudan E. Synthesis and derivatization of near-IR absorbing titanylphthalocyanines with dimethylaminoethylsulfanyl substituents. Dyes Pigm 2007;75:150–5.
[32] Sesalan BS, Koca A, Gül A. Water soluble novel phthalocyanines containing dodeca-amino groups. Dyes Pigm 2008;79:259–64.
[33] Bayir ZA. Synthesis and characterization of novel soluble octa-cationic phthalocyanines. Dyes Pigm 2005;65:235–42.
[34] Karaoğlu HRP, Koca A, Koçak MB. Synthesis, electrochemical and spectroelectrochemical characterization of novel soluble phthalocyanines bearing chloro and quaternizable bulky substituents on peripheral positions. Dyes Pigm 2012;92:1005–17.
[35] Atsay A, Koca A, Koçak MB. Synthesis, electrochemistry and in situ spectroelectrochemistry of water-soluble phthalocyanines. Trans Met Chem 2009; 34:877–90.
[36] Karaoğlan GK, Gümrükçü G, Koca A, Gül A. The synthesis, characterization, electrochemical and spectroelectrochemical properties of a novel, cationic, water-soluble Zn phthalocyanine with extended conjugation. Dyes Pigm 2011;88:247–56.
[37] Gürsoy S, Cihan A, Koçak MB, Bekaroğlu Ö. Synthesis of new metal-free and metal-containing phthalocyanines with tertiary or quaternary aminoethyl substituents. Monatsh für Chem 2001;132:813–9.
[38] Dabak S, Gümüş G, Gül A, Bekaroğlu Ö. Synthesis and properties of new phthalocyanines with tertiary or quaternarized aminoethylsulfanyl substituents. J Coord Chem 1996;38:287–93.
[39] Durmuş M, Nyokong T. Synthesis and solvent effects on the electronic absorption and fluorescence spectral properties of substituted zinc phthalocyanines. Polyhedron 2007;26:2767–76.
[40] Enkelkamp H, Nolte RJM. Molecular materials based on crown ether functionalized phthalocyanines. J Porphyr Phthalocya 2000;4:454–9.
[41] Fu J, Li XY, Ng Dennis KP, Wu C. Encapsulation of phthalocyanines in biodegradable poly(sebacic anhydride) nanoparticles. Langmuir 2002;18:3843–7.
[42] Palchaudhuri R, Hergenrother PJ. DNA as a target for anticancer compounds: methods to determine the mode of binding and the mechanism of action. Curr Opin Biotechnol 2007;18(6):497–503.